

RESEARCH

Open Access



Surgical planning aided with 3D technologies for management of complex paracardiac tumors

Camilo E. Pérez-Cualtán^{1,2}, Catalina Vargas-Acevedo², Juliana Sánchez-Posada¹, Camila Castro-Páez^{1,2}, Roberto Gutiérrez-Vargas^{2,3}, Julián F. Forero-Melo^{2,4}, Juan Manuel Pérez^{2,4}, Juan Carlos Briceño^{1,2}, Héctor M. Medina⁵, Juan Pablo Umaña⁶, Javier Navarro-Rueda^{2,7} and Carlos Eduardo Guerrero-Chalela^{2,8*}

Abstract

Background Accurate diagnosis and treatment of complex cardiac tumors poses challenges, particularly when surgical resection is considered. 3D reconstruction and printing appear as a novel approach to allow heart teams for optimal surgical and post operative care.

Methods We report two patients with uncommon masses including a cardiac angiosarcoma (CAS) and a IgG4-related disease (IgG4-RD) with exclusive cardiac involvement. In both cases, three-dimensional (3D) reconstruction and 3D-printed models were utilized to aid the surgical team achieve optimal pre-operative planning. Both patients underwent ECG-gated cardiac computed tomography angiography (CCTA) imaging and, due to the complex anatomy of the masses, their large dimensions, proximity to vital cardiac and vascular structures, and unclear etiology, computational and 3D-printed models were created for surgical planning. An exploratory literature review of studies using 3D-printed models in surgical planning was performed.

Results In case 1 (CAS), due to the size and extension of the mass to the right ventricular free wall, surgical intervention was not considered curative and, during thoracotomy, an open biopsy confirmed the imaging suspicion of CAS which guided the initiation of optimal medical treatment with chemotherapy and, after clear tumor retraction, the patient underwent a second surgical intervention, and during the 18 months of follow-up showed no signs of recurrence. In Case 2 (IgG4-RD), the patient underwent uncomplicated total surgical resection; this allowed directed treatment and, at 12 months follow-up, there are no signs of recurrence. Computational and 3D-printed models were used to plan the surgery and to confirm the findings. Limited studies have explored the use of 3D printing in the surgical planning of tumors.

Conclusions We present two patients with uncommon cardiac tumors, highlighting the significant value of 3D models in the anatomical characterization and assessment of their extension. These models may be essential in surgical planning for complex cardiovascular cases and could provide more information than conventional imaging modalities. Further studies are needed to demonstrate the impact of 3D technologies in studying cardiac tumors.

*Correspondence:

Carlos Eduardo Guerrero-Chalela
ceguerrero@lacardio.org

Full list of author information is available at the end of the article



© The Author(s) 2024. **Open Access** This article is licensed under a Creative Commons Attribution-NonCommercial-NoDerivatives 4.0 International License, which permits any non-commercial use, sharing, distribution and reproduction in any medium or format, as long as you give appropriate credit to the original author(s) and the source, provide a link to the Creative Commons licence, and indicate if you modified the licensed material. You do not have permission under this licence to share adapted material derived from this article or parts of it. The images or other third party material in this article are included in the article's Creative Commons licence, unless indicated otherwise in a credit line to the material. If material is not included in the article's Creative Commons licence and your intended use is not permitted by statutory regulation or exceeds the permitted use, you will need to obtain permission directly from the copyright holder. To view a copy of this licence, visit <http://creativecommons.org/licenses/by-nc-nd/4.0/>.

Keywords Cardiac tumors, Angiosarcoma, 3D-printing, Surgery

Introduction

The 2021 WHO fifth edition classification of thoracic tumors introduced a revised categorization of cardiac tumors, dividing them into benign types, such as myxomas or hemangiomas, and malignant types, such as angiosarcomas [1]. Cardiac tumors are reported in 6–20% of autopsies, with primary malignant tumors representing only 10% of all cardiac neoplasms [2].

A multimodal approach involving echocardiography, cardiac computed tomography angiography (CCTA), and cardiac magnetic resonance (CMR) is crucial for establishing the diagnosis and treatment of complex cardiac tumors [3]. CT and CMR play a primary role in narrowing down the etiological cause of cardiac masses, as both can assess the tissue composition of cardiac masses, particularly CMR due to its unique ability. Additionally, the high spatial resolution of both techniques enables accurate assessment of size, location, and distances concerning adjacent cardiac and vascular structures [4, 5]. Despite the high accuracy of these techniques for identifying benign lesions, they have limitations for optimal characterization of malignant masses [3].

Surgical resection remains the most effective approach for diagnosing and treating primary cardiac malignancies provided adequate resection margins can be achieved [1, 2]. In cases where surgical resection is deemed necessary, anatomical reconstruction of the structures may be required. Although in 35% of surgical cases, CCTA or CMR scans were crucial for defining the surgical approach, adjustments are needed during surgery, especially when the tumor's edges and morphology are unclear [3]. Three-dimensional (3D) reconstructions have demonstrated higher precision for localization and volume assessment, leading to improved surgical planning, compared to 2D images [4, 5]. 3D printing technologies, including 3D digital reconstructions and printing, are rapidly advancing and modern materials and increasingly sophisticated software for segmentation and 3D reconstruction are being utilized [3]. These advancements within cardiac surgery have enabled a deeper understanding of complex cases, resulting in improved clinical outcomes across various complex cardiac pathologies [6, 7]. There are a rising number of successful surgical treatment of cardiac tumors due to by 3D models utilization for surgical planning, particularly focusing on resection [8–11].

We present two cases involving rare cardiac tumors including a cardiac angiosarcoma (CAS) and immunoglobulin-G4-related disease (IgG4-RD) with exclusive cardiac involvement. In these cases, qualitative and quantitative evaluation of 3D technology aided in the surgical

process. Furthermore, we provide a comprehensive review of 3D printing as a technique to support surgical planning and interventions of cardiac masses.

Methods

Data and ethics statement

Patients' primary and secondary demographic and medical data was collected by informed consents and protocols were approved by the Institutional Review Board and the Ethics Committee at Fundación Cardioinfantil—Instituto de Cardiología (LaCardio, Committee act CEIC-0074-2022, Bogotá, Colombia). The research was conducted in accordance with the Declaration of Helsinki.

Clinical cases

Case 1 -CAS

A 36-year-old woman presented with shortness of breath and marked iron deficiency anemia to an outside hospital. An incidental large mediastinal mass was found during an abdominal CT scan to rule out malignancy as the etiology of her anemia (Fig. 1a-c). Two percutaneous attempts to biopsy the mediastinal mass resulted in acute pericardial hemorrhagic tamponade, requiring emergent drainage. Further evaluations such as trans-thoracic echocardiogram -TTE- (showing a large 96×88 mm mass located at the right atrio-ventricular groove compressing both the right atria and ventricle), CMR (hypo-intensity in T1W, hyperintensity in T2W, no fat saturation, highly vascularized during first pass perfusion and with scattered heterogenous late gadolinium enhancement. After two unsuccessful biopsy attempts, during our multidisciplinary Heart-Team meeting decided to proceed with either partial or complete (if possible) surgical resection to obtain sufficient tissue sample for an accurate histological diagnosis and treatment. To support the surgical approach, a CCTA 3D-printed model was generated.

Case 2 (IgG4-RD)

A 66-year-old male patient with a history of prolonged orotracheal intubation due to Coronavirus-19 infection underwent a chest CT scan for regular follow-up that demonstrated a solid paracardiac mass close to the aortic root and pulmonary trunk, seemingly involving the left coronary artery (Fig. 1d-e). A TTE showed normal biventricular function without significant valvular regurgitation. The CMR confirmed a 28×31 mm mass surrounding the left main coronary artery (LMCA) involving its branches (27 mm extension), displaying specific characteristics: isointensity in T1 and hypointensity in T2W (central early first pass perfusion) with minimal

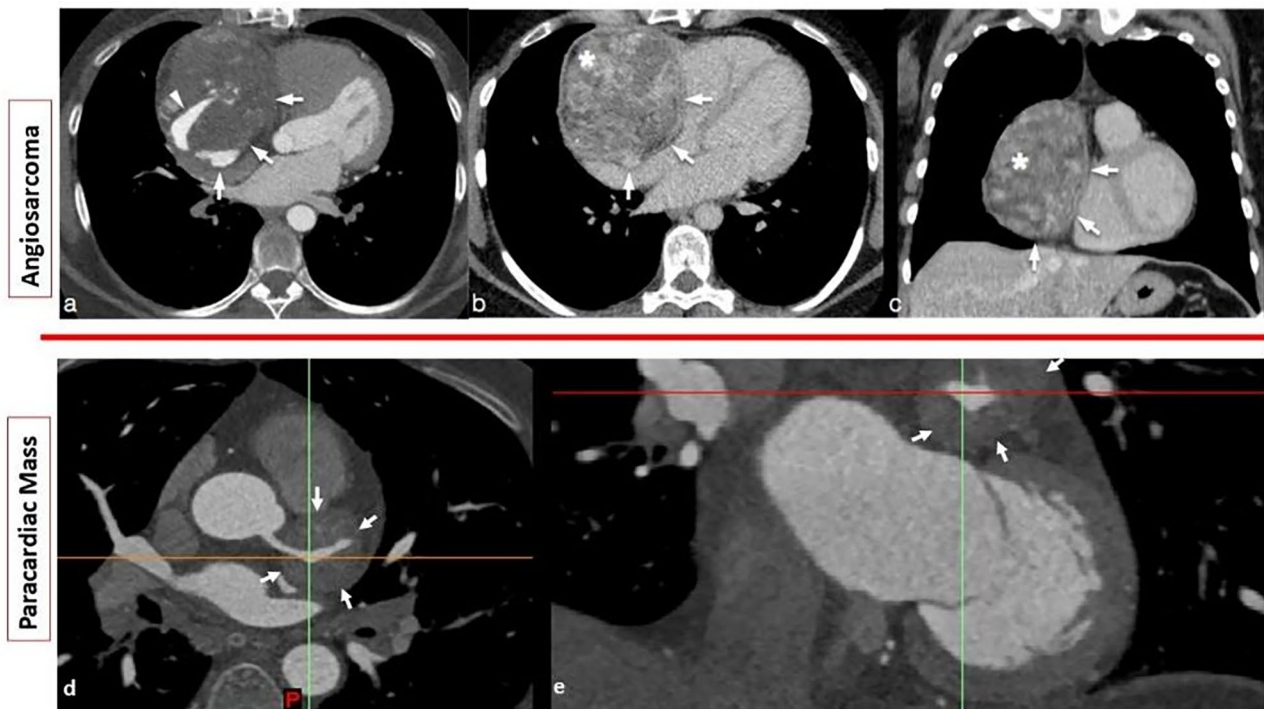


Fig. 1 CCTA images of the two clinical cases to evaluate the contours of the cardiac masses (white arrows) and their relationship to cardiac structures. Patient with angiosarcoma (axial, in **a**, axial, in **b** and coronal, in **c**), where an intense heterogeneous enhancement of the mass is seen (asterisks in **b** and **c**), and the patient with the paracardiac mass (axial, in **d** and coronal, in **e**), where compression of the left coronary artery is seen

peripheral late gadolinium enhancement. Gated CCTA scans revealed distinct contours, mixed density, and focal enhancement, hinting at calcification or hemorrhage. Invasive coronary angiography (ICA) showed left main and proximal descending anterior coronary artery ectasia without occlusion. PET-scan identified heightened metabolic activity within the mass and nearby lymph nodes, suggesting a probable malignancy. The differential diagnosis included Lymphoma, Ormond's disease, or Paraganglioma. Extensive body imaging and blood tests ruled out metastasis, lymphoma, and paraganglioma. Given the uncertainty of the diagnosis and to direct therapy, complete surgical resection was suggested. Due to the complexity of its location near critical cardiac and vascular structures, a 3D-printed model of the heart and the adjacent mass was created for better anatomical assessment.

Image processing and 3D reconstruction

In both cases, to create the patient-specific 3D model reconstruction, an ECG-gated CCTA scan protocol (Siemens SOMATOM-EDGE) was followed to obtain an image size of 512×512 pixels, slice thickness of 0.75 mm, and a slice increment of 0.5 mm, ensuring adequate quality for segmentation. The 3D reconstruction of the anatomy of interest was generated via Mimics Innovation Suite software (Materialise, Inc., Leuven, Belgium).

In case 1 (CAS), the axial venous phase offered the best contrast to delineate the boundaries of the cardiac tumor against the myocardium. A threshold segmentation method based on Hounsfield Units (HU) was employed. Two different thresholds were used to segment the cardiac tissue and the tumor based on the intensities of each structure. Given the similar radiodensity of the tumor to cardiac tissue, the next step involved individually outlining the tumors edges from the left ventricle, right atrium, right ventricle, superior vena cava, and ascending aorta with the aid of the radiology specialist to contrast the threshold segmentation with the imaging expert, acknowledging that using only a threshold system might not be completely reproducible if not guided by an imaging expert. Additionally, to examine tumor vascularity, the arterial phase of the ECG-gated cardiac CCTA scan was used to segment the blood pool of left-sided structures.

For case 2 (IgG4-RD), the left ventricular outflow tract and aorta were isolated. A threshold-based segmentation method was used, and region growth and seed-splitting algorithms were used to separate the structures, considering that the segmentation was a blood pool type. Similarly, to isolate the paracardiac mass, a lower HU threshold was used than that of the cardiac structures, because its radiodensity allowed it. For the coronary arteries, an automatic method was used through the

Coronary tool of the software in which the initial and final landmarks of the arteries in the images were set as input to the algorithm.

After segmentation of the structures of interest, the contours of the 2D images were reconstructed into a 3D stereolithographic file (STL) to generate a 3D digital model, see Fig. 2. In addition, in case 2, further imaging analysis was performed to evaluate the change in compression of the left coronary artery surrounded by the mass. Using the dataset, at 40% of the cardiac cycle (best-systole) and 70% of the cardiac cycle (best-diastole), a 45° cut-in sagittal plane was performed in the LMCA in the 3D models to determine if there were changes in the diameters and area of the transverse section during these two periods of the cycle to analyze by imaging whether

the paracardiac mass compromised the blood flow or if revascularization would be required.

3D printing of anatomical models

The anatomical models generated from medical image segmentation in both cases were exported as 3D reconstructions in STL files, which were then imported into 3D printing software to produce the physical models. For case 1 (CAS), the 3D model was printed (1:2 scale) using polyJet technology on an Objet500/350 Connex3 3D printer (Stratasys, Ltd., MN, USA). Flexible transparent resin (Agilus30, Stratasys, Ltd., MN, USA) was used for the cardiac tissue, and hard magenta resin (VeroMagenta, Stratasys, Ltd., MN, USA) was used for the CAS. For case 2 (IgG4-RD), a two-part model (assembly) was designed to observe the coronary artery within the tumor, and the

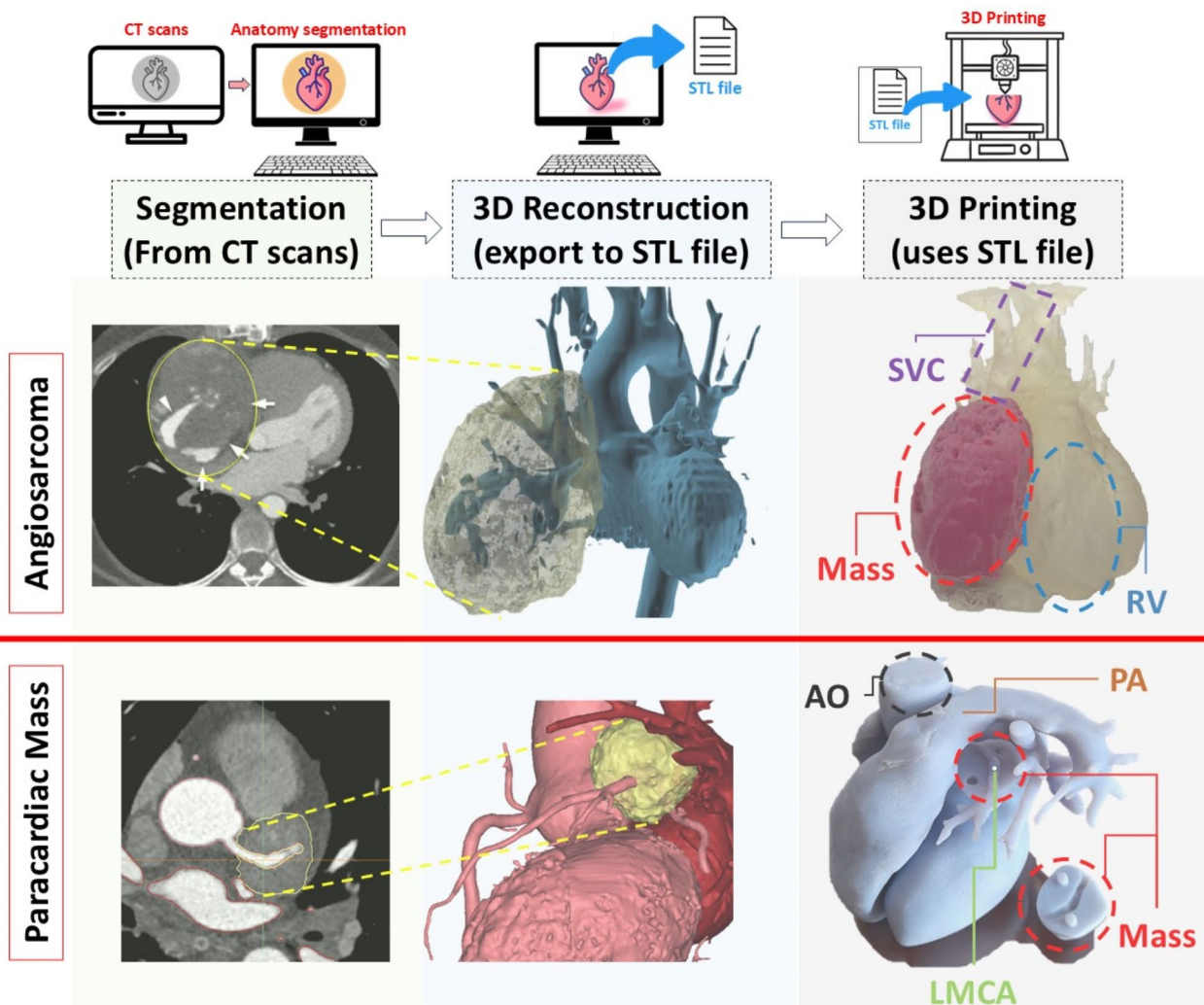


Fig. 2 Method to obtain 3D models of patient-specific anatomy from medical images. (upper row: angiosarcoma and lower row: IgG4-RD paracardiac mass). Segmentation: select the DICOM study dataset from the CT scan and identify and isolate important anatomical structures. 3D reconstruction: the segmented anatomical structures are converted into 3D reconstructions or STL stereolithography files. 3D Printing: The STL files are exported to 3D printing software, in which the material, size and other parameters of the physical models to be highlighted must be selected. In our case we highlight critical cardiac masses, helping in preoperative planning and visualization

entire model was 3D printed (1:1 scale) using PolyJet 3D printing technology with an Objet260 Connex1 printer (Stratasys, Ltd., MN, USA). All model parts were printed with rigid opaque resin (VeroBlue, Stratasys, Ltd., MN, USA).

Review of 3D printing in cardiac tumors

A comprehensive review has been summarized in Table 1 and the study selection process is shown in Fig. 3. The search criterion was set as the earliest date (1985) until January 2024 in cases of tumors and masses in which 3D printing was used for surgical planning. Articles that used only multimodality techniques and 3D reconstruction in CCTA or CMR were discarded since the objective was to study the contribution that new 3D technologies can have in complex cases.

Results

The surgical cases presented here were used to study the role and impact of using 3D models in the clinical workflow. In Case 1, the 3D digital reconstruction and 3D-printed model were delivered to the Heart Team for preoperative planning purposes, and then for postoperative validation of the findings. However, for Case 2, the urgency of the surgery required the early delivery of the 3D digital reconstruction only. The 3D printed model for Case 2 was used postoperatively in a meeting with the surgeon to validate its congruence and relationship with the anatomical findings during surgery.

In case 1, the 3D-printed model was presented to the heart team (Fig. 2). With the model, the surgical team considered there was a clear anatomical correlation between the imaging findings and the macroscopic characteristics of the heart and the tumor tissue on the model. First, the size of the tumor was close to the size of the right ventricle as noticed intra-operatively. Second, the translucent material permitted visualization of the limit of the mass to the collapsed RA posteriorly, the superior vena cava, the AV groove, the ascending aorta and finally, the right ventricle. The biopsy samples collected during the procedure for case 1 used immunohistochemical studies that showed intense and diffuse reactivity in tumor cells were CD31, CD34 and factor VIII and Ki67 index was 10%. Morphologically, the tissue had high fibrous and fibro-adipose components without evidence of cardiac muscle. There was a pattern of an epithelioid neoplasm with many vascular structures lined with endothelial atypical cells due to hyperchromasia with nuclear pleomorphism and focal formation of pseudopapillary and pseudostratified structures (Fig. 4a-d). The morphological characteristics as well as the immunohistochemical pattern were compatible with CAS. Considering the prognosis and the size (98×83 mm) and extension of the mass into the free wall of the right ventricle, the decision

was to not attempt complete surgical resection and rather a partial resection with supportive neoadjuvant chemotherapy (complete cycle of paclitaxel), hoping for cytoreduction and consideration for resection complete if response to therapy. In the follow-up, there was a clear reduction of the mass and no signs of disease extension, the patient underwent a second tumor resection surgery a year later with excellent results and with no immediate perioperative complications; at follow-up at 18 months, the patient continued to have no readmissions and no signs of recurrence.

For case 2 (IgG4-RD), intraoperative findings confirmed the accuracy of the 3D digital reconstruction (Fig. 2), showing the mass surrounding the LMCA and extending to the proximal segments of the left anterior descending (LAD) and left circumflex (LCx) arteries. To ensure complete excision, transection of the ascending aorta, main pulmonary artery, and LMCA was necessary to provide better visualization of the mass. This allowed for the separation of the mass from the aorta, the roof of the left atrium, and the pulmonary artery. The mass excision was completed without complications. Following the removal of the mass, coronary artery bypass surgery was performed using saphenous venous grafts to revascularize the LAD and LCx. Considering the extension of the mass and the compromise of the bifurcation, complete excision of the mass could not be performed without compromising coronary flow. Given the extension of the mass compromise to the LMCA-LAD-LCx, reimplantation was not possible, and bypass grafting was performed to ensure distal coronary flow. It was considered a saphenous vein graft to preserve the possibility of future revascularizations with left internal thoracic artery, considering the absence of coronary artery disease, relatively young age and lifespan of patient. The anatomical information provided by the 3D model to evaluate the congruence of the 3D-printed model and the real mass was fully validated during the surgical procedure. The size of the mass and relationship with the coronary arteries and major vessels were confirmed. As seen in Fig. 5, the difference in the cross-sectional measurement of the real mass (29.88 mm) and the 3D reconstruction (31.90 mm) was 6.76%. There were no perioperative complications and the postoperative period was uneventful, resulting in an early discharge.

The 3D systolic and diastolic reconstructions showed absence of LMCA compression, confirming the results of the ICA (coronary ectasia without significant coronary compression). The diameter and area of the transverse section measured in diastole (4.50×4.04 mm and 14.29 mm²) was greater than the diameter measured in systole (2.91×2.98 mm 6.82 mm²), showing a change in diameter of 45.08%. 3D technologies ensured the coronary artery morphology remained intact, even though the artery was

Table 1 Type of tumor or cardiac mass (2021 WHO classification), location, technology, and material for 3D printing in different studies of cardiac surgery

First Author	Year	Imaging diagnosis	Type of tumor or cardiac mass	Tumor or mass location	Technology and material of the 3D-printed model	Clinical outcome
1 Stephan Jacobs [22]	2008	CT and CMR	Classification: Malignant tumor Coding Heart Tumors: 9120/3 Angiosarcoma	Right ventricular wall and the tricuspid valve	Technology: ColorJet Printing Material: Elastic/Flexible Multicolor Technique: full heart model to assemble with myocardium, with echocardiographic section for evaluation of the right ventricle, tumor and great vessels in different color. They used a single material apparently.	Postoperatively the echocardiography showed properly the size of the right ventricle with no obstruction of the Right Ventricular Outflow Tract. No follow-up reported later.
2 Schmauss Daniel [23]	2013	Ultrasonography, CT and CMR	Classification: Malignant tumor Coding Heart Tumors: 8810/0 Fibroma	Right ventricular wall	Technology: Fusion Deposition Modeling Material: Rigid Multicolor Technique: full heart hollow model model with myocardium, and the fibroma was printed in a different color. They used a single material apparently.	No patient outcome reported.
3 Kuk Hui Son [19]	2015	Trans-thoracic echocardiography, CT and CMR	Classification: Benign tumor Coding Heart Tumors: 8810/0 *Neurofibroma	Interatrial septum	Technology: Fusion Deposition Modeling Material: Rigid Multicolor Technique: full heart model model of the type of blood-pool, with the mass in a different color. They used a single material apparently.	The postoperative coronary artery CT showed clear resection margin. The patient was discharged without complication. No follow-up reported later.
4 Odeaa Al Jabbari [24]	2016	CT and CMR	Patient 1: Malignant tumor *Mesenchymal Tumors of the Thorax – Osteosarcoma Patient 2: Malignant tumor *Post-renal cell carcinoma – encapsulated mass	Patient 1: Left atrium and mitral valve Patient 2: Right atrium and the inferior vena cava	Technology: White Jet Process (similar to PolyJet) Material: Elastic/Flexible and rigid Multicolor Technique: for both cases, models were printed only of the structure related to the tumor (atriums i.e.). Hollow wall model and with a cross-sectional view. The cardiac masses were printed in a different color. They used elastic material for the wall and rigid material for the tumors apparently.	P1 & P2: After surgery, pathology report showed negative surgical margins. At six-month follow-up, the patients do not present tumor recurrence.
5 Kyle W Riggs [18]	2018	Echocardiography, CT and CMR	Patient 1: Benign tumor Coding Heart Tumors: 8840/0 Myxoma Patient 2: Benign tumor Coding Heart Tumors: 8900/0 Rhabdomyoma	Patient 1: Right Coronary Artery and Right Ventricle Patient 2: Left Coronary Artery and Left ventricle	Technology: PolyJet Material: Elastic/Flexible and rigid Multicolor Technique: full heart model model of the type of blood-pool, with the cardiac mass in a different color and material. They used elastic material for the hollowed tumor and rigid material for the cardiac structures.	P1: The patient was discharged without complication. CMR performed at 6 months postoperatively revealed that the remaining tumor was necrosing and regressing in size. At 2 years, there were no echocardiographic or CMR findings of left ventricular wall motion abnormality. P2: No tumor was resected in the mitral valve annulus. The patient remained on ECMO and developed a lung infection. After 2 weeks, the patient died of multi-organ failure.
6 Menegazzo Willian R. [25]	2019	Echocardiography and CT	Classification: Malignant tumor Coding Heart Tumors: 9120/3 Angiosarcoma	Left atrium	Technology: Not specified Material: Not specified Technique: structure related to the tumor (left atrium i.e.). The tumor was printed in a different color. They used elastic material for the solid model (left atrium) and rigid material for the tumor apparently.	Complete tumor resection was accomplished. At one-year follow-up, he remains functionally well and free of local recurrence.

Table 1 (continued)

First Author	Year	Imaging diagnosis	Type of tumor or cardiac mass	Tumor or mass location	Technology and material of the 3D-printed model	Clinical outcome
7 Mojahid Ali [26]	2020	Trans-thoracic echocardiography, CT and CMR	Classification: Benign tumor Coding Heart Tumors: 8840/0 Myxoma	Superior vena cava	Technology: stereolithography Material: Rigid Multicolor Technique: full heart model of the type of blood-pool to assemble, with the left side in red, right side in blue and the tumor in yellow. They used a single material apparently.	The patient was discharged without complication except for the development of sick sinus syndrome that required a pacemaker. At one-year follow-up, a cardiac CT showed no tumor recurrent.
8 Zhou Yang-zhao [27]	2021	Trans-thoracic echocardiography and CT	Classification: Benign tumor Coding Heart Tumors: 8840/0 Myxoma	Left atrium	Technology: stereolithography Material: Rigid Multicolor Technique: full heart solid model of the type blood-pool, with each structure in different color (including the tumor). They used a single material apparently.	The patient was discharged without complication. At one-year follow-up, no recurrent tumor was found or any arthymias.

*Not classified as a cardiac tumor or mass.

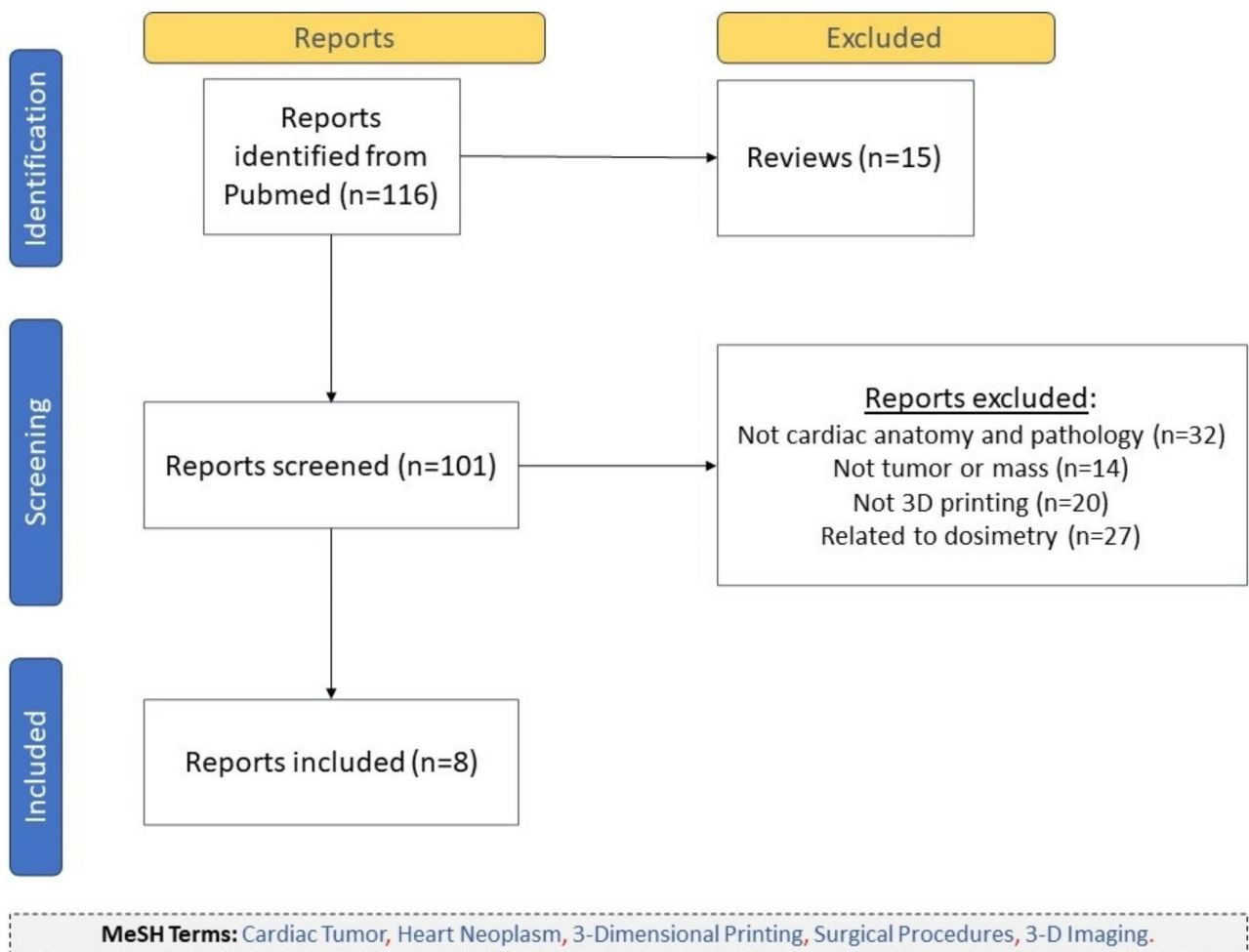


Fig. 3 Selection of studies for inclusion of the review by January 2024

surrounded by the mass at all phases of the cardiac cycle (Fig. 6).

The anatomopathological specimen revealed a mononuclear cell infiltrate with lymphocytes, macrophages,

and abundant plasmatic cells, all embedded in a fibrotic stroma with a focally storiform arrangement (Fig. 4e-f). Immunohistochemical studies showed reactivity in a plasma cell population for both IgG and IgG4, with a 50%

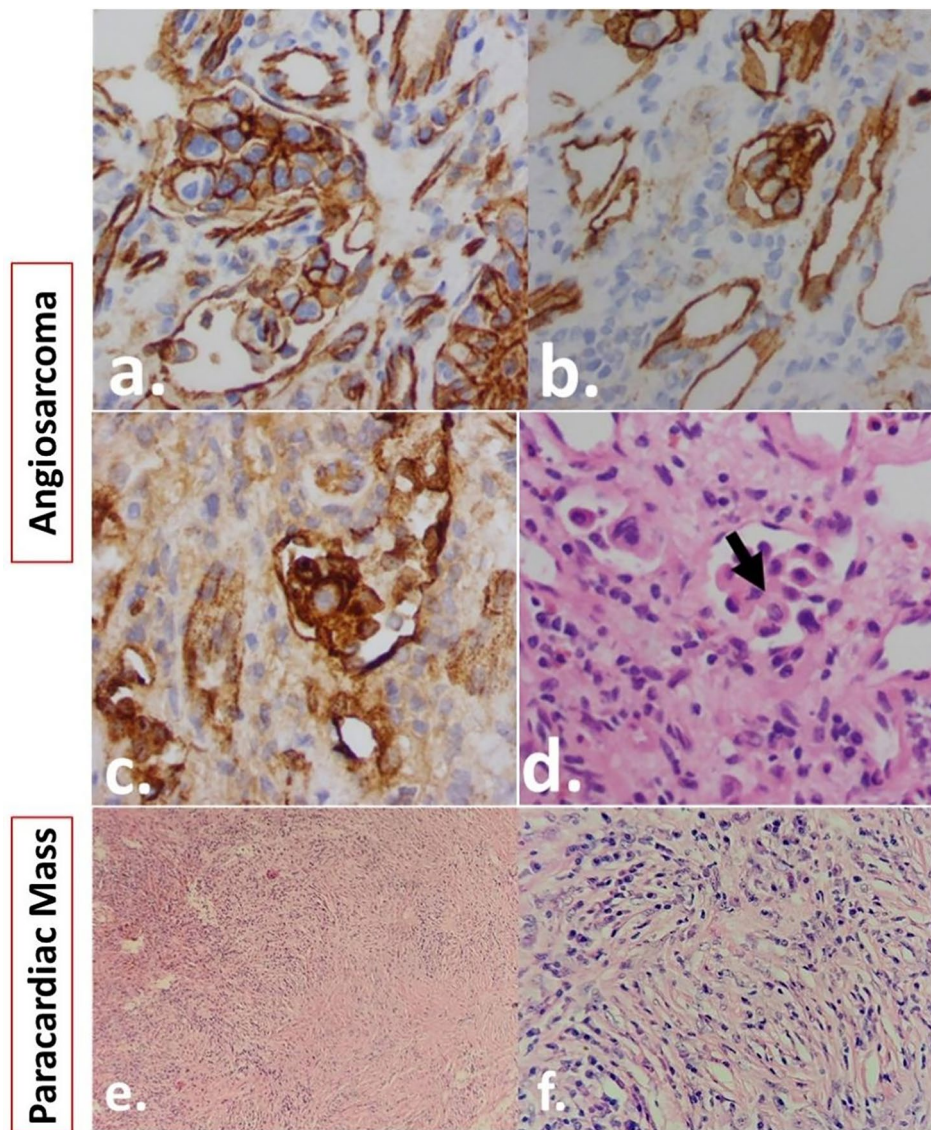


Fig. 4 Biopsy results (upper rows: angiosarcoma and lower row: paracardiac mass). **(a)** Immunohistochemical studies show reactivity to CD31, **(b)** CD34 and **(c)** factor VIII, and **(d)** view of the tumor, endothelial cells, vascular structures, and cellular atypia (arrow shows formation of pseudopapillary structure), **(e)** 10x histopathological visualization of the resected paracardiac mass and **(f)** 40X augmented visualization

IgG4+/IgG+ratio, and focal areas contained over 100 IgG4-positive plasma cells per high-power field, indicative of a dense infiltrate of IgG4-positive plasma cells, confirming the diagnosis of IgG4-related disease (IG4-RD). Treatment, based on prednisolone and methotrexate, was initiated with good short- and mid-term results. At 12 months follow-up there were no signs of IgG4-RD extension and TTE revealed normal biventricular function with no regional wall motion abnormalities and a post-operative CCTA showed no recurrence of cardiac or mediastinal lesions, peritoneal extension and absence paratracheal or hilar nodes.

Review results

The review showed 8 studies in which 3D-printed models were used for surgical planning (Table 1). The mean age of the adult patients was 47 ± 15 years; 75% were female, and two patients were pediatric: a 2-month-old female and a 12-day-old male. 70% of the patients had cardiac tumors (classification 2021WHO), mostly myxomas (Cardiac Tumor Coding: 8840/0), followed by angiosarcomas (Cardiac Tumor Coding: 9120/3), and 30% of the remaining tumors originated in adjacent extracardiac structures and involved the heart. However, they are not classified as primary cardiac tumors. The 3D-printed models were used in cases in which there was not

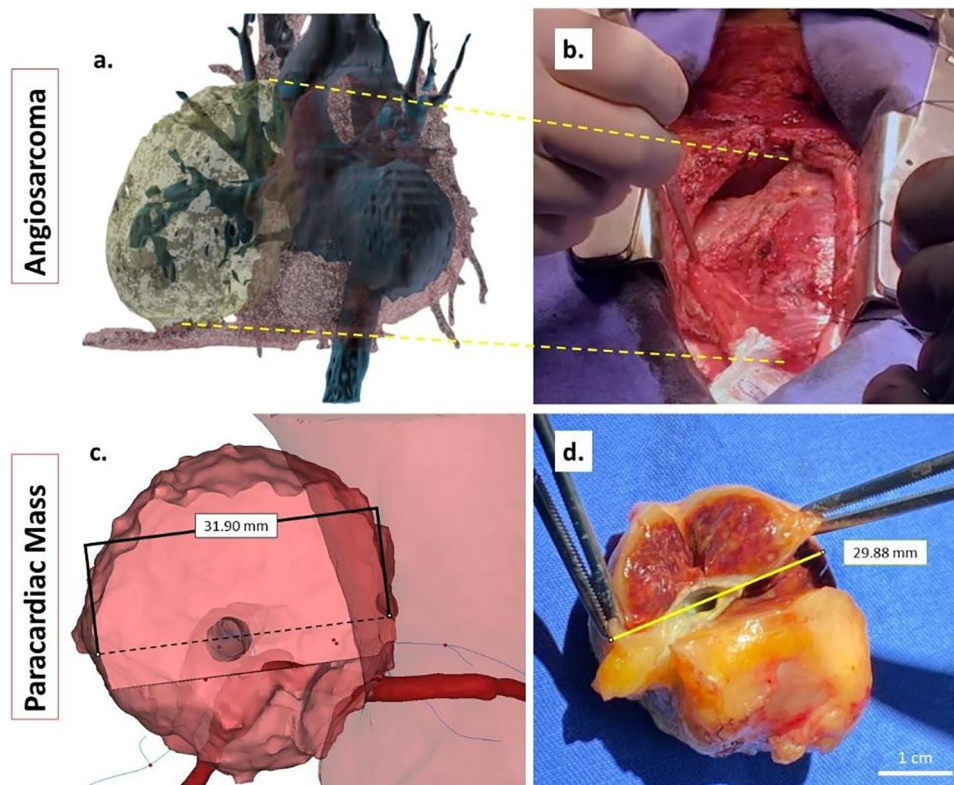


Fig. 5 (a) 3D Reconstruction of the angiosarcoma and (b) surgical finding, and (c) 3D reconstruction of case 2, IgG4-RD, showing the path and center line of the left coronary artery and (d) resected mass specimen with the respective coronary involvement

complete certainty or clarity of the resection margins or in cases in which other cardiac structures were involved.

Discussion

We present two cases of paracardiac tumors involving a CAS (case 1) and an IgG4-RD (case 2), with the latter being the sole manifestation of the disease. Despite utilizing a multimodal imaging approach, and given the complexity of the cases, a multidisciplinary team planned the surgical procedures utilizing 3D models. The 3D models provided extensive information about the margins between the masses and cardiac tissue, aiding in directed treatment in case 1 and resection in case 2.

Cardiac tumors are rarely encountered in day-to-day cardiology practice, with an incidence of 1,380 per 100 million individuals [12]. Tumors can be categorized as either neoplastic or non-neoplastic. Among neoplastic tumors, secondary tumors or metastases are significantly more common, being up to 132 times more frequent than primary tumors [8]. Furthermore, primary cardiac tumors are predominantly benign (90%), with only a small proportion being malignant (10%) [13, 14].

The approach requires a multimodal imaging evaluation, including echocardiography, CCTA, and CMR. However, a biopsy is mandatory for proper diagnosis chambers and to the right coronary artery, due to its

habitual location, resection is often impossible [15]. Therefore and treatment in many cases, especially in suspected malignant lesions, with complete surgical resection recommended in certain cases. Alongside CMR, CCTA presents a favorable diagnostic option for identifying calcified masses and examining thoracic morphology and associated vascular structures [6]. The clinical approach requires a multimodal imaging evaluation, including echocardiography, CCTA, and CMR, although in some cases more is needed, and the use of new technologies is required [7].

Cardiac sarcomas, particularly cardiac angiosarcomas (CAS), constitute the majority of primary malignant tumors of the heart, with around 40% of cases reported in case series [9, 10]. They are typically located at the right atrium in 75% of cases [7]. Surgical resection confers the best long-term outcomes; however, considering the high likelihood of metastasis at presentation and infiltration to right sided chambers and to the right coronary artery, due to its habitual location, resection is often impossible [15]. Therefore, neoadjuvant chemotherapy with debulking may often be the treatment of choice. For case 1, macroscopic evaluation confirmed the 3D model findings. It allowed the surgical to approach a sequential surgical resection with partial tumor excision aided with neoadjuvant chemotherapy, this due to the evidence of

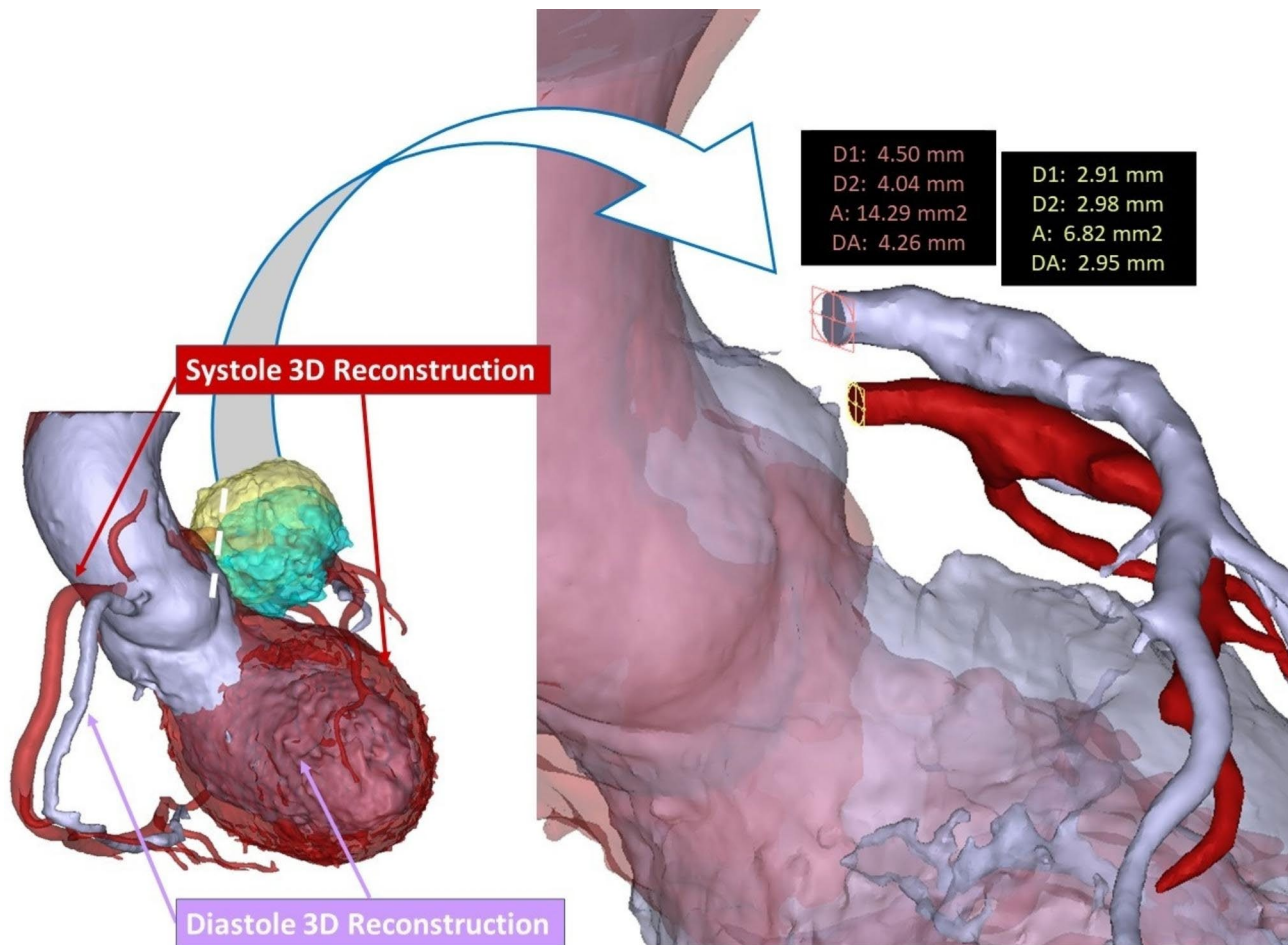


Fig. 6 Dimensional change analysis of the left coronary artery in the 3D model compromised by the IgG4RD paracardiac mass, showing no significant left main coronary artery compression by this simulation

large size and extent of the tumor infiltrating the right ventricular free wall, in which a complete excision in the first attempt was deemed impossible without safely preserving vital structures (Fig. 5a) with a high risk of vascular complications and ventricle laceration. At follow-up, one year after therapy, it was decided to resect the tumor and 18 months later the patient has no local recurrence or related symptoms.

IgG4-RD is known to cause fibroinflammatory lesions in nearly any organ system. However, diagnostic criteria established by the American and European League Against Rheumatism do not include cardiac involvement as a criterion its diagnosis [11]. Cardiac manifestations can vary widely, including pericarditis, myocarditis, valvular heart disease, cardiac masses, and coronary involvement [16]. Early recognition of cardiac manifestations is crucial for initiating directed management and treatment, potentially reducing disease extension, as cardiac involvement may precede systemic manifestations when detected early [17]. Coronary involvement, characterized by the “mistletoe sign,” is reported in up to 15.4% of cases

and can present with coronary stenosis or aneurysms in 65% and 40% of cases, respectively, often leading to symptomatic presentations such as coronary syndromes [16]. The “mistletoe sign” is characterized by a perivascular mass surrounding the coronary artery (See Fig. 4), resembling the mistletoe plant attached to the three branches, albeit rare its clinical utility lies that it serves as a characteristic of IgG4-RD, and therefore aid diagnosis of this rare condition directing treatment [18]. Moreover, it might serve as a follow-up marker as reports have shown remission of this sign with directed treatment [18].

In case 2, the mass was found to be incidental, with no involvement of other organs, despite extensive evaluation. Considering its broad differential diagnosis and close relationship to vital structures, we generated a 3D model in printed and digital forms to corroborate the surgical approach. A 3D-printed model was created, separating the vital structures with the mass cut in half to demonstrate LMCA involvement; this approach helps to show the typical “mistletoe sign” coronary involvement

as shown in Fig. 2. Finally, a dynamic simulation revealed that the mass did not compromise this vessel, as predicted by the 3D digital assessment and as shown by ICA (Fig. 4).

In recent years, alongside the described multimodal approach, 3D printing technologies have been widely employed in complex cardiovascular scenarios [19]. The 3D models allow the Heart-Team to explore the location, size, and relationship between critical structures and surrounding tissues. Moreover, selecting the 3D printing materials is important and, in our cases, it depends on the surgeon's requirements. For the two cases, two different 3D printing techniques were used; in the first case, the CAS was printed using color and flexibility to distinguish between the tumor (rigid magenta) from the other cardiac structures (flexible translucent). For the second case, the entire heart (cardiac structures and mass) was printed in the same material and color (light blue). However, for case 2 the model was designed and printed as an assembly to observe possible compression of LMCA and the typical characteristic of cardiac involvement in IgG4-RD. The approach used for both cases was to highlight the mass or tumor, with color, elasticity, or as a separate part. From the surgeon's perspective, in both cases, differentiating the region of interest (tumor or mass) with color visually aids in evaluation and planning, as other studies have also reported [13, 14].

The 3D models generated from patient-specific data provide our surgical team with insight into real anatomical dispositions and relationships, helping to identify potential complications and develop a unique treatment strategy prior to the operation [20]. However, only a few reports have provided insights into 3D printing and modeling in cardiac tumors. According to search results, in 2008, the first 3D-printed case of a cardiac tumor for surgical planning was reported. After 2015, an incremental trend was seen in the reported studies, presumably due to the use of 3D printing in other surgical practices and easier access to 3D printers [10, 11, 13, 14, 19–22].

Out of the 8 studies identified in the literature search, three did not report patient follow-up beyond 6 months or local tumor recurrence, while four studies (6/10 patients) provided follow-up data beyond 6 months or 1 year, showing no local recurrence. In only one of the reviewed papers the patient died, which was considered related to the severity of the disease [23]. Most reports utilized 3D models to assess tumor limits, extension, and involvement with cardiac vital structures [19, 21, 22]. Moreover, in some cases, there could be a contraindication to surgery due to an estimated 50% mortality rate based on 2D images [10]. Additionally, the models confirmed the surgical approach and procedure (resection and auto-transplantation), while others indicated a change in the access site [24, 25], or the initial surgical

plan [26]. Each study emphasizes a specific variable in the planning process elucidated by using 3D models, such as tumor access site, anatomical position and relationship, unique identification of cardiac structures, or tumor invasion and involvement of surrounding vital structures. It is essential to relate these variables associated with the model, such as the color of structures to highlight tumor extent or to use flexible materials for resection and suturing, as experimented in some reports [22, 27]. As seen in case 2, in scenarios involving tumors and cardiovascular surgery, the focus is not only on generating 3D reconstructed image models but also on guiding the medical team to facilitate optimal decision-making.

Although most studies highlight the positive impact of 3D models on understanding tumor anatomy and surgical planning, the lack of data on model accuracy and direct surgical outcomes limits objective evaluation. Some studies suggest improvements in surgical outcomes, but conclusive evidence of clinical benefits remains sparse. Additionally, the accuracy of 3D-printed models compared to surgical findings relies heavily on the segmentation process. In case 2, we aimed for a more objective approach by measuring the cross-sectional area of the paracardiac mass in the 3D reconstruction and comparing it to the extracted mass (see Fig. 5). Recognizing the limitations of the segmentation process and the paucity of data on the accuracy of 3D models in comparison with surgical findings, as shown in our literature review, there is a clear need for prospective studies with standardized evaluation criteria to accurately assess the efficacy and clinical impact of 3D printed models in cardiac surgery.

Regarding the segmentation software, interestingly, all studies utilizing 3D-printed models for preoperative planning of tumors or cardiac masses employed specialized software for 3D segmentation and reconstruction, particularly the Mimics Innovation Suite software (Materialise, Inc., Leuven, Belgium). However, more clinical studies are needed to contrast the impact of printed models with control groups, comparing intraoperative variables (e.g., surgery time, medical devices used) and postoperative outcome variables (e.g., mortality, hospitalization, follow-up longer than 1 year), which can also be utilized for cost-effectiveness studies.

The use of 3D printing and/or new technologies for preoperative planning of cardiac tumors is increasing in the literature. However, there is still a tendency to report only case studies, presumably because a prospective study of uncommon cases can be time-consuming. However, more studies with significant samples and their associated clinical and economic impact are anticipated. Finally, we employed the WHO classification for cardiac tumors to standardize the nomenclature of cases, facilitating comparison and exchange of information in for further investigations [27].

Conclusions

We present two cases where 3D printing and modeling contributed to decision-making and surgical planning for rare cardiac tumors. Given the rarity of each disease presentation and their close anatomical relationship to vital structures, a comprehensive resection attempt was made with the assistance of 3D models. These models may offer additional information regarding the boundaries between cardiac tumors and vital cardiac and vascular structures, insights that 2D images may not provide. Further studies are necessary to fully understand the role of 3D printing in studying and improving surgical outcomes for cardiac tumors.

Supplementary Information

The online version contains supplementary material available at <https://doi.org/10.1186/s13019-024-03096-w>.

Supplementary Material 1

Acknowledgements

The authors would like to acknowledge the Heart Team, the Department of Cardiovascular Surgery, the Department of Research at Fundación Cardioinfantil – Instituto de Cardiología (Bogotá, COL) and the Department of Biomedical Engineering at Universidad de los Andes (Bogotá, COL).

Author contributions

Camilo E. Pérez-Cualtán: Engineering team; Conceptualization; Methodology; Data curation; Review analysis; Segmentation and 3D printing; Formal analysis; Writing—original draft; Writing—review & editing. Catalina Vargas-Acevedo: Medical team; Conceptualization; Methodology; Data curation; Formal analysis; Writing—original draft; Writing—review & editing. Juliana Sánchez-Posada: Engineering team; Methodology; Segmentation; Formal analysis; Writing—original draft. Camila Castro-Páez: Engineering team; Conceptualization; Methodology; Data curation; Review analysis; Formal analysis; Writing—review & editing. Roberto Gutiérrez-Vargas: Medical team; Methodology; Data curation; Formal analysis. Julián F. Forero: Imaging team; Conceptualization; Methodology; Data curation; Formal analysis; Writing—original draft. Juan Manuel Pérez: Medical team; Conceptualization; Methodology; Data curation; Formal analysis; Writing—original draft. Juan Carlos Briceño: Engineering team; Conceptualization; Methodology; Data curation; Review analysis; Formal analysis; Writing—review & editing. Hector M. Medina: Imaging team; Conceptualization; Methodology; Data curation; Formal analysis; Writing—original draft. Juan Pablo Umaña: Surgical team; Conceptualization; Methodology; Data curation; Formal analysis; Writing—original draft. Javier Navarro-Rueda: Engineering team; Conceptualization; Methodology; Data curation; Review analysis; Segmentation and 3D printing; Formal analysis; Writing—original draft; Writing—review & editing. Carlos Eduardo Guerrero-Chalela: Medical team; Conceptualization; Methodology; Data curation; Review analysis; Segmentation and 3D printing; Formal analysis; Writing—original draft; Writing—review & editing.

Funding

The project involving the Center for Modeling and 3D Printing at Fundación Cardioinfantil – LaCardio (Bogotá, Colombia) and the development of the anatomical models is funded by the Colombian Ministry of Science – MinCiencias (Ministerio de Ciencia, Tecnología e Investigación) under contract 744–2021 (Project code #223989785090).

Data availability

No datasets were generated or analysed during the current study.

Declarations

Ethics approval

Informed consents and protocols were approved by the Institutional Review Board and the Ethics Committee at Fundación Cardioinfantil—LaCardio (FCl-IC, Bogotá). The research was conducted in accordance with the Declaration of Helsinki.

Consent for publication

The manuscript is not submitted for publication or consideration elsewhere.

Competing interests

The authors declare no competing interests.

Author details

¹Department of Biomedical Engineering, Universidad de los Andes, Bogotá, Colombia

²Center for 3D Modeling and Printing, Fundación Cardioinfantil – LaCardio, Bogotá, Colombia

³School of Medicine, Universidad del Rosario, Bogotá, Colombia

⁴Department of Radiology and Diagnostic Imaging, Fundación Cardioinfantil – Instituto de Cardiología, Bogotá, Colombia

⁵Department of Cardiac Imaging, The Texas Heart Institute, Baylor College of Medicine, Houston, TX, USA

⁶Department of Cardiac Surgery, Cleveland Clinic, Weston, FL, USA

⁷Department of Industrial Engineering, Pontificia Universidad Javeriana, Bogotá, Colombia

⁸Fundación Cardioinfantil – Instituto de Cardiología, Calle 163A # 13B - 60 Bogotá, Bogotá 1113111, Colombia

Received: 12 June 2024 / Accepted: 15 September 2024

Published online: 28 September 2024

References

1. Ambrus N et al. Feb., Primary cardiac angiosarcoma: A case report, *Echocardiography*, vol. 35, no. 2, pp. 267–271, 2018, <https://doi.org/10.1111/echo.13808>
2. Maleszewski JJ et al. The 2021 WHO classification of tumors of the heart. Apr 01 2022 Elsevier Inc <https://doi.org/10.1016/j.jtho.2021.10.021>
3. Mitsouras D et al. Nov., Medical 3D printing for the radiologist, *Radiographics*, vol. 35, no. 7, pp. 1965–1988, 2015, <https://doi.org/10.1148/rg.2015140320>
4. Xenogiannis I et al. Aug., Saphenous Vein Graft Failure: From Pathophysiology to Prevention and Treatment Strategies, *Circulation*, vol. 144, no. 9, pp. 728–745, 2021, <https://doi.org/10.1161/CIRCULATIONAHA.120.052163>
5. Back L, Ladwiniec A. Saphenous Vein Graft Failure: Current Challenges and a Review of the Contemporary Percutaneous Options for Management, Nov. 01, 2023, *Multidisciplinary Digital Publishing Institute (MDPI)*. <https://doi.org/10.3390/jcm12227118>
6. Gaisendrees C, et al. Benign and malignant cardiac masses: long-term outcomes after surgical resection. *Expert Rev Anticancer Ther.* 2022. <https://doi.org/10.1080/14737140.2022.2116006>.
7. Tyebally S et al. Cardiac tumors: JACC CardioOncology State-of-the-art review. Jun 01 2020 Elsevier Inc <https://doi.org/10.1016/j.jaccao.2020.05.009>
8. Oliveira GH, Al-Kindi SG, Hoimes C, Park SJ. Characteristics and survival of malignant cardiac tumors a 40-year analysis of > 500 patients. *Circulation.* 2015;132(25):2395–402. <https://doi.org/10.1161/CIRCULATIONAHA.115.016418>.
9. Kumari N, et al. Primary Cardiac Angiosarcoma: a review. *Cureus Jul.* 2023. <https://doi.org/10.7759/cureus.41947>.
10. Ramlawi B, et al. Surgical Treatment of primary cardiac sarcomas: review of a single-Institution experience. *Ann Thorac Surg.* Feb. 2016;101(2):698–702. <https://doi.org/10.1016/j.athoracsur.2015.07.087>.
11. Matsumura I, et al. IgG4-related disease with a Cardiac Mass. *Intern Med.* 2020;59(9):1203–9. <https://doi.org/10.2169/internalmedicine.4054-19>.
12. Cresti A, et al. Incidence rate of primary cardiac tumors: a 14-year population study. *J Cardiovasc Med.* 2016;17(1):37–43. <https://doi.org/10.2459/JCM.0000000000000059>.
13. Riggs KW, Dsouza G, Broderick JT, Moore RA, Morales DLS. 3D-printed models optimize preoperative planning for pediatric cardiac tumor debulking,

- Transl Pediatr*, vol. 7, no. 3, pp. 196–202, Jul. 2018, <https://doi.org/10.21037/tp.2018.06.01>
14. Son KH et al. Nov., Surgical planning by 3D printing for primary cardiac schwannoma resection, *Yonsei Med J*, vol. 56, no. 6, pp. 1735–1737, 2015, <https://doi.org/10.3349/ymj.2015.56.6.1735>
 15. Meng Q, Lai H, Lima J, Tong W, Qian Y, Lai S. Echocardiographic and pathologic characteristics of primary cardiac tumors: a study of 149 cases, 2002. [Online]. Available: www.elsevier.com/locate/ijcard
 16. Fragoulis GE, Evangelatos G, Tektonidou MG. Vasculitis beyond aortitis in IgG4-related disease (IgG4-RD): case report and review of the literature. Mar 01 2021 Springer Sci Bus Media Deutschland GmbH. <https://doi.org/10.1007/s10067-020-05302-1>
 17. Soh BWT, et al. Severe aortic valvular incompetence from IgG4-Related disease: an unusual entity. *JACC Case Rep*. Oct. 2023;24. <https://doi.org/10.1016/j.jaccas.2023.102027>.
 18. Xu X, et al. Remission of ‘mistletoe sign’ after treatment. *J Cardiovasc Comput Tomogr*. Nov. 2020;14(6):e118–9. <https://doi.org/10.1016/j.jcct.2019.08.002>.
 19. Meyer-Szary J et al. Mar., The Role of 3D Printing in Planning Complex Medical Procedures and Training of Medical Professionals—Cross-Sectional Multispecialty Review, *Int J Environ Res Public Health*, vol. 19, no. 6, 2022, <https://doi.org/10.3390/ijerph19063331>
 20. Liddy S, McQuade C, Walsh KP, Loo B, Buckley O. The Assessment of Cardiac masses by Cardiac CT and CMR Including pre-op 3D Reconstruction and Planning. Sep 01 2019 Curr Med Group LLC. <https://doi.org/10.1007/s11886-019-1196-7>
 21. Sun Z, Wee C. 3D Printed Models in Cardiovascular Disease: An Exciting Future to Deliver Personalized Medicine, Oct. 01, 2022, *MDPI*. <https://doi.org/10.3390/mi13101575>
 22. Jacobs S, Grunert R, Mohr FW, Falk V. Work in progress report - Experimental. 3D-Imaging of cardiac structures using 3D heart models for planning in heart surgery: A preliminary study, *Interact Cardiovasc Thorac Surg*, vol. 7, no. 1, pp. 6–9, Feb. 2008, <https://doi.org/10.1510/icvts.2007.156588>
 23. Zhou YZ, Tang T, Luo C, Zhou XM, Fu XM. Case Report: 3D Printing guided Cardiac Autotransplantation for treatment of a giant Complex Primary Left Atrial Tumor. *Front Cardiovasc Med*. 2021;8. <https://doi.org/10.3389/fcvm.2021.800459>.
 24. Al Jabbari O, Abu Saleh WK, Patel AP, Igo SR, Reardon MJ. Use of three-dimensional models to assist in the resection of malignant cardiac tumors. Sep 01 2016 Blackwell Publishing Inc <https://doi.org/10.1111/jocs.12812>
 25. Menegazzo WR, et al. Modified autotransplant with three-dimensional printing for treatment of primary cardiac sarcoma. *J Thorac Cardiovasc Surg*. Feb. 2019;157(2):e41–3. <https://doi.org/10.1016/j.jtcvs.2018.08.087>.
 26. Ali M, Pham AN, Pooley RA, Rojas CA, Mergo PJ, Pham SM. Three-dimensional printing facilitates surgical planning for resection of an atypical cardiac myxoma, *J Card Surg*, vol. 35, no. 10, pp. 2863–2865, Oct. 2020, <https://doi.org/10.1111/jocs.14896>
 27. Schmauss D, Gerber N, Sodian R. Three-dimensional printing of models for surgical planning in patients with primary cardiac tumors. Mosby Inc. 2013. <https://doi.org/10.1016/j.jtcvs.2012.12.030>.

Publisher's note

Springer Nature remains neutral with regard to jurisdictional claims in published maps and institutional affiliations.